
Article:
Wilkinson, R.N., Koudijs, M.J., Patient, R.K. et al. (3 more authors) (2012) Hedgehog signaling via a calcitonin receptor-like receptor can induce arterial differentiation independently of VEGF signaling in zebrafish. Blood, 120 (2). pp. 477-488. ISSN 0006-4971

https://doi.org/10.1182/blood-2011-10-383729

Published in final edited form as:
Blood. 2012 July 12; 120(2): . doi:10.1182/blood-2011-10-383729.

Hedgehog signalling via a calcitonin receptor-like receptor can induce arterial differentiation independently of VEGF signalling in zebrafish

Robert N. Wilkinson[1,2], **Marco J. Koudijs**[3], **Roger K. Patient**[4], **Philip W. Ingham**[1,2], **Stefan Schulte-Merker**[3,4], and **Fredericus J.M. van Eeden**[1,2]

[1]MRC Centre for Developmental and Biomedical Genetics, University of Sheffield.

[2]Department of Biomedical Sciences, University of Sheffield.

[3]Hubrecht Institute – KNAW & University Medical Centre Utrecht.

[4]MRC Molecular Haematology Unit, Weatherall Institute of Molecular Medicine, University of Oxford

[5]Experimental Zoology Department, Wageningen University.

Abstract

Multiple signalling pathways control the specification of endothelial cells (ECs) to become arteries or veins during vertebrate embryogenesis. Current models propose that a cascade of Hedgehog (Hh), Vascular Endothelial Growth Factor (VEGF) and Notch signalling acts instructively on ECs to control the choice between arterial or venous fate. Differences in the phenotypes induced by Hh, VEGF or Notch inhibition suggest that not all of the effects of Hh on arterial-venous specification, are mediated by VEGF. We establish that full derepression of the Hh pathway in *ptc1;ptc2* mutants converts the posterior cardinal vein into a second arterial vessel that manifests intact arterial gene expression, intersegmental vessel sprouting and haematopoietic stem cell (HSC) gene expression. Importantly, whilst VEGF was thought to be absolutely essential for arterial fates, we find that normal and ectopic arterial differentiation can occur without VEGF signalling in *ptc1;ptc2* mutants. Furthermore, Hh is able to bypass VEGF to induce arterial differentiation in ECs via the calcitonin receptor-like receptor, thus revealing a surprising complexity in the interplay between Hh and VEGF signalling during arteriovenous specification. Finally, our experiments establish a dual function of Hedgehog during induction of *runx1*$^{+}$ HSCs.

Introduction

Amongst the first fully differentiated cells to arise in the vertebrate embryo are the mesodermally derived haematopoietic and endothelial lineages, which comprise the circulatory system, itself the first functional organ system to develop. Unravelling the signalling networks that govern the formation of the vasculature has taken on added significance with the recent demonstration of the emergence of haematopoietic stem cells (HSCs) from ventral endothelium of the dorsal aorta (DA) [1-3]. In zebrafish, haematopoietic and endothelial lineages arise from a common bipotential progenitor, the haemangioblast [4].

Corresponding author: Freek van Eeden, MRC Centre for Developmental and Biomedical Genetics/Dept. Biomedical Sciences, Western Bank, Sheffield. S10 2TN Tel: +44 114 222 2348 f.j.vaneeden@sheffield.ac.uk.

Authorship RNW designed research, performed research, analysed data and wrote the paper. MK designed research, performed research, analysed data. FJMvE designed research, analysed data and wrote the paper. PWI, RKP, SSM discussed the data and edited the paper.

Europe PMC Funders Author Manuscripts

Haemangioblasts are specified within ventral mesoderm, alongside unipotential haematopoietic progenitors and angioblasts. These three cell types are transported via the cellular rearrangements and morphological movements of gastrulation to reside as two bilateral cell populations within the lateral plate mesoderm. The first major vessels of vertebrate embryos form via vasculogenesis, whereby migratory angioblasts coalesce to generate lumenised vessels. In zebrafish, angioblasts within the posterior lateral mesoderm (PLM) migrate medially beneath the somites and coalesce ventral to the notochord and hypochord at the midline. These cells form the major trunk vessels, the DA and PCV [5].

The exact regulation and timing of endothelial specification is an important developmental question, but published data are currently difficult to reconcile. A genetic basis for arterial and venous differentiation was established with the identification of Ephrin-B2 and EphB4 receptors as markers of arteries and veins respectively [6,7]. Using lineage tracking, clusters of ECs were identified within the zebrafish PLM, which either contributed to the DA or PCV, but never both, leading to the suggestion that determination of arterial and venous fate within ECs occurs prior to angioblast migration [8]. The molecular basis of this proposed fate restriction is unclear since differential expression of known arterial or venous markers (*ephrinb2a*, *kdrl and flt4*) is observed after the migrating angioblasts arrive at the midline [9-11]; however, the first angioblasts to reach the midline and contribute to the DA express activated ERK during their migration [12]. Importantly, recent studies show that some *flk1/kdrl*$^{+}$(arterial) angioblasts migrate ventrally and contribute to the PCV following their arrival at the midline [13]. Taken together, these studies suggest endothelial progenitors are specified as arterial or venous prior to circulation, but it is unclear whether they are fully determined prior to migration to the midline.

The Notch signalling pathway is a key determinant in the establishment of arterial identity [9]. In mice, Notch receptors and ligands exhibit arterially restricted expression and targeted inactivation of Notch pathway components results in defective arterial specification[14]. Zebrafish mindbomb (*mib*) mutants, which are defective for Notch signalling, exhibit arterial-venous shunts, defective PCV formation and reduced arterial gene expression, whilst gridlock (*grl*) mutants, which contain a lesion in *hey2*, exhibit reduced arterial gene expression and DA maturation defects [9,15,16].

Whilst Notch signalling guides arterial fate, elegant studies in zebrafish and more recently in mouse, revealed Hh and VEGF signalling to act upstream of Notch in arterial specification [17,18]. Zebrafish *sonic-you* (*syu*) mutants, which lack midline Shha activity, exhibit a drastic reduction in arterial gene expression. This failure to specify the DA correctly was proposed to result from failure to express *vegfa* in the adjacent somites [17]. How this transcriptional activation occurs has not been addressed. Recently, a study positioned Crlra downstream of Hh signalling and upstream of VEGF within this hierarchy but the precise molecular details remain unclear [19]. Whatever the exact mechanism of VEGF induction, *vegfa* morphants exhibit reduced arterial gene expression, whilst *vegfa* overexpression induces ectopic arterial differentiation and can rescue the loss of arterial differentiation in *syu* mutant embryos, indicating its indispensability [17]. VEGF binds to Kdrl or Kdr, a receptor tyrosine kinase, thereby activating downstream Phospholipase C gamma1 (Plcg1) [20]. Zebrafish *kdrl* and *plcg1* mutants are defective in arterial but not in venous specification [21,22]. Less is known about venous determination; in mouse, active repression of Notch signalling may occur in venous ECs [23]. In zebrafish, PI3K signalling downstream of VEGF may maintain venous identity via its ability to block MAPK signalling, which itself favours arterial differentiation via activation of ERK [12].

Hh signalling inhibition in zebrafish embryos results in a failure to form two distinct trunk axial vessels, a phenotype more severe than in embryos lacking VEGF signalling, implying

that additional components act downstream of Hh to regulate arterial differentiation [9,17,20]. Consistent with this, ectopic lumenised vessels can be induced by exogenous Shh but not by VEGF [24]. Differences in the response of ECs to Hh and VEGF may account for this [25], however, recent studies in mammals have revealed VEGF-independent roles for Hh signalling in vascular lumenisation, yet the underlying mechanism remains unclear [18]. In zebrafish, activation of Hh signalling can induce arterial differentiation at the expense of venous identity [26]; here, we extend these findings through analysis of animals doubly mutant for the Hh receptors Ptc1 and Ptc2, which exhibit constitutive activation of Hh signalling [27,28]. We show that Hh induces arterial differentiation at the expense of venous fate, effectively converting the PCV into a second DA, which displays intact arterial expression in addition to arterial characteristics, such as precocious vessel sprouting and HSC gene expression. In addition, we show that in *ptc1;ptc2* mutants, arterial differentiation can occur independently of VEGF signalling, via a parallel pathway whereby Hh signalling acts via Crlra to induce arterial differentiation. Given the high conservation of these genetic hierarchies between zebrafish and mammals, the identification of Crlr signalling in parallel with VEGF may account for the VEGF-independent effects of Hh signalling during mammalian arterial development [18].

Materials and Methods

Zebrafish husbandry

Zebrafish (*Danio rerio*) embryos from wild-type, *ptch1*^{hu1602}/+;*ptch2*^{tj222}, *smo*^{hi1640Tg}/+, *plcg1*^{t26480}/+, Tg(*fli1a:EGFP*)*y1*/+, Tg(*gata1:dsred*)*sd2*/+ strains were raised at 28.5°C as described [29].

Drug treatments

Purmorphamine (Chemistry Research Laboratory, South Parks Rd, Oxford, United Kingdom; stock solution in DMSO: 2.5mg/ml) was used as previously described [30]. SU5416, Cyclopamine (Merck; stock solution 10mM in DMSO & 95% ethanol, respectively) were used in E3 medium at a concentration of 2μM from tailbud and 50μM from high stage, respectively.

Whole-mount RNA *in situ* hybridisation

Experiments were performed as previously described [11]. Myc expression was detected using anti-c-Myc primary antibody (9E10) (AbCam) (1:500) alongside anti-DIG antibody. Embryos were incubated with Alexa-Fluor® 488 secondary antibody (Invitrogen) (1:200) and imaged, followed by developing of *in situ* staining.

Crlra overexpression constructs

Full length *crlra* was amplified by RT-PCR with the SuperScript™ One-Step RT-PCR System (Invitrogen) using the primers 5′-ggatcccgctccggtactctgacatc-3′, 5′-ctcgagcacattgccatgttgagtgg-3′. The resulting BamHI/XhoI fragment was cloned into pCS2+. Capped mRNA was generated using mMessage Machine® SP6 Kit (Ambion).

In situ probes

wnt16 probe was amplified using the primers 5′-cctttgtgctctcagggaag-3′, 5′-gcgttgctctttatccttgc-3′ and cloned into pGem®-T-Easy (Promega). *crlra* probe was created via PCR generated from IMAGE:7141310 (Source Bioscience) using primers 5′-tggataaccgtattaccgcc-3′, 5′-cgcgcaattaaccctcactaaagcactagtcataccaggatc-3′.

Fli1:Myc-dnPKA:IRES-EGFP construct

Construct was generated using the Tol2 kit via standard methods [31]and the following components; Fli1 enhancer/promoter, P5efli1EP [32], BamHI-XbaI fragment of pSP64T-PKI [33] p3EIRES-EGFPpA [31]. Embryos were injected at 1 cell stage with 25ng/ul Tol2 mRNA and Fli1:Myc-dnPKA:IRES-EGFP DNA.

Morpholino injections

Embryos were injected with 1nl *crlra* morpholino (Gene Tools) (0.67mM dissolved in distilled water) 5′-agctcgctgtcatcttctttggcat -3′ [19]; 0.5nl (0.5mM) *Su(H)* morpholino 5′-caaacttccctgtcacaacaggcgc-3′ [34]; 0.5nl (10ug/ul) *kdr* morpholino 5′-gttttcttgatctcacctgaaccct-3′[22]; 0.5nl (10ug/ul) *kdrl* morpholino 5′-ccgaatgatactccgtatgtcacctt-3′[35].

Confocal imaging

Confocal images were collected using a Leica DM IRE2 microscope. Time-lapse confocal images were collected using a PerkinElmer Ultraview Vox microscope. Images were analysed using Volocity® to reconstruct a 3D representation.

Results

Zebrafish *ptc1*;*ptc2* mutants show defective angioblast migration and fail to establish circulation

Although both *ptc1* heterozygous and homozygous embryos exhibit increased levels of Hh signalling, vascular development is not obviously affected in either, and the circulatory loop is established normally. Similarly, *ptc2* homozygotes have no detectable defects in the circulatory system [28]. However, double mutant *ptc1*;*ptc2* embryos, which exhibit constitutive Hh signalling, by contrast, failed to establish circulation, resulting in pooling of primitive erythrocytes in the intermediate cell mass and posterior blood island (Fig. 1A, B, red arrowhead). This was further confirmed using the Tg(*fli1a:EGFP*)*y1* and Tg(*gata1:dsred*)*sd2* transgenes [36,37] to visualise both developing vasculature and primitive erythrocytes at onset of circulation. Using time-lapse confocal microscopy, we observed that in wild-type embryos, primitive erythrocytes entered circulation via the PCV, as previously described [13] (Fig. 1E, yellow arrowhead and Movie S1), whereas, in *ptc1*;*ptc2* embryos, they failed to enter the circulation, mainly residing within the PCV (Fig. 1F, yellow arrowhead and Movie S2). Double mutant embryos also exhibit disorganised vasculature. In wild-type embryos at 26hpf, the DA and PCV were juxtaposed following the entry of primitive erythrocytes into circulation (Fig. 1E), whilst in *ptc1*;*ptc2* mutants, the two axial vessels were clearly separated (Fig. 1F). In more anterior regions, at 27 hpf, *ptc1;ptc2* embryos exhibited a drastic reduction of endothelial *cdh5* staining in the duct of Cuvier (Fig. 1C, D, black arrowheads), and the adjoining PCV (Fig. 1C, D, white arrowheads) indicating these vessels were absent, which would explain the failure to establish a circulatory loop in *ptc1;ptc2* double mutants.

The medial migration of angioblasts is regulated by Hh signalling [11,26]; thus, to investigate whether a migration defect could contribute to the failure to form proper vessels, we used the Tg(*fli1a:EGFP*)*y1* transgene to follow medial migration of blood and endothelial progenitors in live *ptc1*;*ptc2* embryos (Fig. 1G-L). In control Tg(*fli1a:EGFP*)*y1*/+ embryos, GFP^+ angioblasts migrated such that by 12s, the first GFP^+ DA angioblasts had reached the midline (Movie S3 and Fig. 1G, white arrowhead). By 15s, these cells had begun to coalesce into a vascular cord at the midline (Fig. 1H, white arrowhead), closely followed by angioblasts, which contribute to the PCV (Fig. 1H, yellow arrowheads). By 18s, the vascular cord extended posteriorly (Fig. 1I, white arrowhead), whilst some angioblasts remained

more lateral and had not yet reached the midline (Fig. 1I, yellow arrowheads). In Tg(*fli1a:EGFP*)*y1*/+;*ptc1*;*ptc2* embryos, by contrast, quantification using ImageJ revealed a 38% decrease in GFP^+ cells throughout the embryo at 12s and 55% fewer angioblasts migrated towards the midline at this stage (Movie S4 and Fig. 1J, white arrowheads), such that by 15s, 43% fewer angioblasts had reached the midline, forming a discontinuous vascular cord (Fig. 1K, white arrowheads) with many angioblasts present in more lateral positions (Fig. 1K, yellow arrowheads). By 18s, the vascular cord extended anteroposteriorly in Tg(*fli1a:EGFP*)*y1*/+;*ptc1*;*ptc2* embryos, yet remained discontinuous and contained fewer GFP^+ cells along the A-P axis (Fig. 1I, K, white arrowheads). Many GFP^+ cells also remained in more lateral positions at 18s in Tg(*fli1a:EGFP*)*y1*/+;*ptc1*;*ptc2* embryos (Fig. 1L yellow arrowheads). Thus, aberrant migration could contribute to the observed circulation defect. We also examined the effect of Hh signalling deficiency on angioblast migration using Tg(*fli1a:EGFP*)*y1*/+;$smo^{hi1640Tg}$ embryos [38]. In contrast to recent studies [26], we observed that angioblasts in Tg(*fli1a:EGFP*);$smo^{hi1640Tg}$ embryos migrated in two waves, yet failed to coalesce into an endothelial cord at the midline (Movie S6 and Fig. S1D-F). Taken together, these results suggest that either elevated or absent Hh signalling results in impaired angioblast migration, implying that the levels of Hh signalling perceived by angioblasts is important in their successful migration to the midline.

More detailed analysis of angioblast migration for a period of 17 hours from 16 somite stage revealed that whilst the vasculature formed normally in Tg(*fli1a:EGFP*)*y1*/+ embryos (Movie S7), Tg(*fli1a:EGFP*)*y1*/+;*ptc1*;*ptc2* embryos exhibited delayed formation of the DA, resulting from aberrant medial migration of angioblasts, however, the DA ultimately formed a continuous vessel in these embryos (Movie S8). Importantly, no angioblasts were observed to migrate ventrally and contribute to the PCV, as described previously [13]. Furthermore, in Tg(*fli1a:EGFP*)*y1*/+;*ptc1*;*ptc2* embryos, angioblasts in the position of the PCV in the posterior trunk were observed to migrate dorsally and contribute to the nascent DA (Movie S8). VEGF has been shown to limit the ventral migration of angioblasts [13], thus, in *ptc1;ptc2* mutants, where VEGF signalling is elevated (Fig. 3L, green arrowhead), angioblasts migrated dorsally to contribute to the dorsal aorta, thereby underlining the importance of VEGF signalling as a directional cue in this process.

ptc1;*ptc2* mutants exhibit ectopic arterial differentiation at the expense of venous differentiation, resulting in conversion of the PCV into an arterial vessel

During normal development, intersegmental vessels (ISVs) sprout from the DA from 24hpf onwards, whilst venous ISVs sprout later between 1.5dpf and 2dpf [39,40]. In *ptc1*;*ptc2* embryos, by contrast, precocious ISV formation was clearly observed in the PCV at 27hpf (Fig. 2B, C, D white arrowheads), suggesting that the PCV had acquired arterial characteristics. Optical sectioning and 3D reconstruction confirmed that the sprouting ISVs originated from the PCV and not the DA (Fig. 2F, white arrowhead). In addition to the precocious PCV sprouts, *ptc1;ptc2* mutants displayed atypical endothelial connections between the DA and PCV (Fig. 2B, grey arrowheads), which were not present in control embryos (Fig. 2A, C).

To evaluate the differentiation status of the vessels in *ptc1*;*ptc2* embryos, we assayed arterial and venous marker gene expression by *in situ* hybridisation. Expression of the VEGF receptor *kdrl* normally exhibits an arterial bias, originally being present throughout the nascent vasculature, but becoming downregulated in the PCV and restricted to the DA by 26-27hpf (Fig. 3A, red arrowhead). In *ptc1*;*ptc2* mutants, by contrast, *kdrl* expression is maintained in the PCV during vascular development (Fig. 3A, B, blue arrowheads). Whilst the arterial marker *ephrinb2a* was ectopically expressed in the PCV (Fig. 3C, D, blue arrowhead), the expression of *aplnra* in venous endothelium [41], was absent or substantially downregulated in the PCV of *ptc1*;*ptc2* mutants (Fig. 3E, F, blue arrowheads). Furthermore,

expression of the VEGF receptor *flt4*, which is restricted to the PCV at 27hpf, was substantially downregulated in *ptc1*;*ptc2* mutants (Fig. 3G, H, blue arrowheads). Ectopic arterial gene expression in the PCV of *ptc1*;*ptc2* mutants, combined with a loss of venous gene expression indicates that the PCV had undergone a fate change and was converted into an artery. We also assessed the onset of arterial gene expression within the *ptc1;ptc2* mutants and did not observe any induction of arterial markers within pre-migratory angioblasts (data not shown), however, ectopic expression of the arterial marker *dll4* was observed as early as 18s (Fig. S2A, B, red arrowheads) and was detectable in angioblasts which had not yet reached the midline in *ptc1;ptc2* mutants (Fig. S2D, asterisks). Similarly, precocious midline expression of *ephrinb2a* was observed at 18s (Fig. S2E-H, red arrowheads) and 19s (Fig. S2I-L, red arrowheads) in *ptc1;ptc2* embryos. Thus, activation of Hh can change both spatial and temporal profile of arterial gene expression.

Analysis of *runx1*$^{+}$ HSCs in *ptc1;ptc2* embryos confirms conversion of the PCV to an arterial vessel, and indicates a dual function of Hh in their induction

Expression of the transcription factor *runx1*, is normally restricted to cells in the ventral DA and also marks emerging definitive haematopoietic progenitors and HSCs [11,42,43]. In *ptc1:ptc2* mutants, *runx1* was expressed ectopically in the PCV, supporting the hypothesis that the PCV had acquired arterial character (Fig. 3J, black arrowheads). Quantification of the number of *runx1*$^{+}$ cells in *ptc1;ptc2* mutants revealed an 89% reduction (Fig. S3) and these cells were absent from the DA (Fig, 3I, J, white arrowheads). Recent studies have revealed a novel signalling pathway in the zebrafish somite [44], whereby somitic *wnt16* signalling upstream of *deltaC/deltaD* was necessary for initiation of *runx1* expression within the DA. Since *ptc1;ptc2* embryos exhibit somite patterning defects, we analysed *wnt16* expression and found that it was persistently reduced in the somites of *ptc1;ptc2* mutant embryos from 10s onwards (Fig. 4A-D black arrowheads). In line with this, expression of *deltaD* was lost within the somitic mesoderm from 10s (Fig. 4G, H black arrowheads), as was *deltaC* (Fig. 4E, F; [27]. That *runx1* is expressed at all is surprising given the early downregulation of *wnt16* and *deltaC/deltaD*, however, we have previously demonstrated that *bmp4* expression is required for initiation of *runx1* expression in the DA ([30]. Furthermore, *ptc1;ptc2* mutants exhibit strong upregulation of *bmp4* within the pronephric ducts (data not shown). It is therefore possible that Bmp signalling is able to rescue the loss of somitic *wnt16-DeltaC/D* by inducing *runx1* expression within arterial ECs close to the source of *bmp4*. Taken together, these data indicate that ectopic Hh signalling affects *runx1*$^{+}$ HSCs in two opposing ways: first by promoting arterial fate in the ventral vessel allowing ectopic HSCs to form, but at the same time antagonising somitic *wnt16* and *deltaC/D*, leading to a reduction in overall HSC numbers.

The level of Hh and VEGF signalling determines the balance between venous and arterial fates

Since Hh sits atop a signalling hierarchy that activates VEGF [17,19], we analysed *vegfa* expression in *ptc1*;*ptc2* mutants and found it was significantly up-regulated throughout the trunk of mutant embryos (Fig. 3K, L, green arrowheads), consistent with previous studies [7]. We also treated wild-type embryos with the Smoothened agonist Purmorphamine (PMA) from tailbud stage onwards [45], since PMA is capable of activating Hh signalling to a greater level than that observed in *ptc1* mutants, but less than that of *ptc1;ptc2* mutants [30]. PMA treated embryos demonstrated increased *kdrl* and *ephrinb2a* expression within the DA (Fig. S4A-D, red arrowheads). PMA treated embryos also retained higher *kdrl* expression within the PCV (Fig. S4A, B blue arrowheads), whilst *ephrinb2a* was not ectopically induced. In contrast to *ptc1;ptc2* mutants, PMA treated embryos exhibited a moderate increase in *vegfa* expression (Fig. S4G, H) and expression of the venous marker *aplnra* was considerably reduced or absent in the PCV of PMA treated embryos (Fig. S4E, F, blue arrowheads).

Taken together, these results indicate that the levels of Hh signalling and subsequent *vegfa* expression are critical for the balance between arterial versus venous differentiation.

Arterial specification occurs independently of VEGF signalling in *ptc1;ptc2* mutants

Upregulated *vegfa* expression in *ptc1*;*ptc2* mutants (Fig. 3K, L, green arrowheads) implies that the aberrant PCV specification was due to an increase in VEGF signalling. To address this, we crossed the *plcg1*^{t26480} mutant [40], which blocks VEGF signalling downstream of its receptor [20] into the *Tg(fli1a:EGFP)y1*/+;*ptc1;ptc2* background. Whilst the vasculature of Tg(*fli1a:EGFP*)*y1*/+ siblings exhibited normal ISV sprouting (Fig. 5A), ectopic ISVs were observed in Tg(*fli1a:EGFP*)*y1*/+;*ptc1;ptc2* embryos (Fig. 5B). Furthermore, whereas the axial vessels were juxtaposed in Tg(*fli1a:EGFP*)*y1*/+ embryos (Fig. 5A), the two vessels could be observed discretely in Tg(*fli1a:EGFP*)*y1*/+;*ptc1;ptc2 embryos* (Fig. 5B). In contrast, no ISVs were present in Tg(*fli1a:EGFP*)*y1*/+;*plcg1* embryos, indicating defective angiogenesis arising from inhibition of VEGF signalling (Fig. 5C) [20,46,47]. Whilst ISVs were absent in Tg(*fli1a:EGFP*)*y1*/+;*ptc1;ptc2;plcg1* embryos (Fig. 5D, E), the developing vasculature consisted of a non-continuous dorsal vessel, which was not closely juxtaposed to the ventral vessel. Expression of *kdrl* at 27hpf was reduced in the PCV (Fig. 5F blue arrowhead) of Tg(*fli1a:EGFP*)*y1*/+ sibs and retained in the DA (Fig. 5F, red arrowhead) and ISVs (Fig. 5F, yellow arrowhead). In contrast, ectopic *kdrl* expression was retained in both vessels in Tg(*fli1a:EGFP*)*y1*/+;*ptc1;ptc2;plcg1* mutant embryos (Fig. 5G, red arrowheads). Consistent with this, arterial *ephrinb2a* was retained in all Tg(*fli1a:EGFP*)*y1*/+;*ptc1;ptc2;plcg1* embryos and demonstrated punctate expression throughout the trunk in the position of the dorsal and ventral vessels (Fig. 5I, red arrowheads). Both *kdrl* and *ephrinb2a* are strongly downregulated in *plcg1* mutants [36].

Although the *ptc1;ptc2;plcg1* triple mutant is expected to have no VEGF signalling, bifurcations in the downstream signalling cascade imply that the use of alternative effectors cannot be excluded. To control for this possibility, we employed an inhibitor of VEGF signalling, SU5416, which acts at the level of the VEGF receptor, [48,49]. We treated the progeny of Tg(*fli1a:EGFP*)*y1*/+;*ptc1*/+;*ptc2*/+ × *ptc1*/+;*ptc2*/+ crosses, with high concentrations of SU5416 (2 μM) from tailbud stage to ensure maximal inhibition of VEGF signalling (Fig. S5). In treated *ptc1*;*ptc2* mutants, expression of arterial markers such as *dll4* and *ephrinb2a* were retained, albeit with reductions in the number of arterial ECs (Fig. S5h, l, red arrowheads) relative to DMSO treated *ptc1;ptc2* mutants (Fig. S5F, J, red arrowheads). However, in SU5416 treated siblings, all arterial differentiation was absent (Fig. S5E, G, I, K, red arrowheads). Moreover, ectopic arterial differentiation was retained in SU5416 treated *ptc1*;*ptc2* mutants (Fig. S5H, L, red arrowhead). These results indicate that activation of Hh signalling can induce arterial differentiation independently of VEGF signalling.

This result was surprising given previously demonstrated requirements for VEGF in arterial differentiation. However, it remains formally possible that the levels of SU5416 used, which were determined by its non-specific toxicity at higher doses, were insufficient to inhibit elevated VEGF signalling in *ptc1*;*ptc2* embryos. To address this issue, we asked whether the same dose of SU5416 was sufficient to inhibit the effects of exogenous *vegf*$_{121}$ mRNA. Embryos were injected with 50pg *vegfa* mRNA, more than 2x higher concentration than that sufficient to induce substantial ectopic arterial differentiation [17]. As expected, embryos injected with *vegf*$_{121}$ mRNA and treated with DMSO exhibited ectopic *ephrinb2a* expression throughout the trunk (Fig. S6B, red arrowhead). By contrast, 63% of injected embryos treated with SU5416 exhibited total loss of *ephrinb2a* in the trunk (Fig. S6D, red arrowhead), whilst the remaining 37% exhibited weak expression and no ectopic *ephrinb2a* expression was observed (data not shown). These data clearly indicate that the concentration of SU5416 employed is sufficient to inhibit very high levels of VEGF signalling.

As a further control, we co-injected *ptc1;ptc2* mutant embryos with morpholinos targeting the VEGF receptors *kdr* and *kdrl* [22,35], which together are required to transduce the VEGF signal. Combinatorial knock-down abolished arterial *ephrinb2a* expression in non-double mutant sibs (Fig. S7A, C; red arrowhead). By contrast, *ptc1;ptc2* mutant embryos retained ectopic *ephrinb2a* expression (Fig. S7D, red arrowhead), although no vessel sprouting was observed and fewer *ephrinb2a*$^{+}$ cells were present (Fig. S7B, red arrowhead).

Finally, to demonstrate endothelial cell autonomy of Hedgehog signalling, we mosaically activated Hedgehog signalling within ECs by co-injecting a Fli1:Myc-dnPKA:IRES-EGFP DNA construct and Tol2 mRNA into embryos which were treated with cyclopamine, to inhibit Hedgehog signalling and downstream VEGF (Fig. S8). Murine dnPKA is a well-established activator of Hedgehog signalling [33]. Uninjected embryos treated with cyclopamine displayed a total absence of the early and late arterial markers *dll4* (Fig. S8I, J, black arrowheads) and *ephrinb2a* within the vasculature (Fig. S8D, F, black arrowheads; and [11]). By contrast, injected embryos treated with cyclopamine exhibited ECs co-expressing Myc-dnPKA and *dll4* (Fig. S8G, H, arrowheads) and *ephrinb2a* (Fig. S8K, L, arrowheads). This rescue of arterial differentiation indicates that Hedgehog signalling is able to act cell autonomously in ECs. Taken together, our triple mutant analysis, SU5416 exposure, VEGF receptor knock-down and demonstration of cell autonomy all show that high levels of Hh signalling are able to induce arterial differentiation in a VEGF-independent manner.

Arterial specification in *ptc1;ptc2* mutants is dependent upon Notch signalling

To determine whether loss of Notch, which acts downstream of VEGF, could prevent ectopic arterial differentiation in *ptc1;ptc2* embryos, we injected a morpholino targeting *Su(H)* [34], a protein essential for Notch signal transduction [50]. Knockdown of *Su(H)* in non-double mutant sibling embryos resulted in blood vessels (Fig.6A, B yellow arrowheads) which failed to express arterial *ephrinb2a* (Fig. 6C, D, red arrowheads). Interestingly, knockdown of *Su(H) in ptc1;ptc2* double mutant embryos also resulted in a total loss of vascular *ephrinb2a* expression (Fig. 6E, F red arrowheads). These data indicate that the VEGF-independent signalling in *ptc1;ptc2* embryos occurs upstream of Notch.

Knockdown of *crlra* in combination with VEGF inhibition prevents arterial differentiation in *ptc1*;*ptc2* mutants

Our finding that arterial differentiation can occur independently of VEGF signalling but is dependent upon Notch, raises the important question of how Hh is able to bypass VEGF to activate downstream target genes. We evaluated *crlra*, a downstream target of Hh with a role in arterial induction [19]. In wild-type embryos, *crlra* was diffusely and weakly expressed throughout the somites (Fig. 7A, green arrowhead) but also weakly expressed in the DA (Fig. 7A, red arrowhead). Conversely, in *ptc1;ptc2* embryos, *crlra* was considerably upregulated both in the somites (Fig. 7B, green arrowhead) and in the DA (Fig. 7B, red arrowhead). Thus increased Crlra might account for the retention of arterial differentiation in VEGF inhibited *ptc1*;*ptc2* mutants.

Embryos were injected with *crlra* morpholino [19] and treated with SU5416. As previously described, SU5416 treated wild-type embryos revealed a total absence of arterial differentiation within the trunk vasculature (Fig. 7G, K; red arrowhead). In *ptc1;ptc2* mutants, by contrast, treatment with SU5416 was unable to block arterial *ephrinb2a* expression (Fig. 7H, L: blue arrowhead). Wild-type embryos injected with *crlra* morpholino exhibited considerable downregulation of *ephrinb2a* (Fig. 7G, I, red arrowhead), whilst those injected with *crlra* morpholino and treated with SU5416 displayed a total absence of *ephrinb2a* throughout the trunk vasculature (Fig. 7M, red arrowhead). However, knockdown

of *crlra* in *ptc1;ptc2* embryos failed to prevent induction of *ephrinb2a*, which was expressed ectopically (Fig. 7J, blue arrowhead). In *ptc1;ptc2* embryos, only combined knockdown of *crlra* and VEGF inhibition by SU5416 resulted in a total loss of *ephrinb2a* within the trunk vasculature (Fig. 7N, red arrowhead).

A confounding aspect of the latter experiment is that *crlra* normally activates somitic VEGF expression [19], so morpholino knock-down of *crlra* would be expected to lead to downregulation both of Crlra and VEGF. To address whether activation of Hh can bypass this function of Crlra, we assayed *vegfa* expression in *ptc1;ptc2* mutant embryos and found that in non-double mutant siblings, knockdown of *crlra* resulted in a decrease in somitic *vegfa* expression (Fig. 7C, D, arrowhead) as previously reported [19]. However, in *ptc1;ptc2* mutants, *crlra* knockdown produced no observable difference in *vegfa* expression (Fig. 7F, arrowhead) relative to uninjected *ptc1;ptc2* mutants (Fig. 7E, arrowhead). We conclude that Hh is indeed able to signal in parallel to Crlr to induce expression of *vegfa*. Taken together with our observations that Notch signalling is required for arterial differentiation in *ptc1;ptc2* mutant embryos, these data indicate that Hh signalling is capable of inducing arterial differentiation via Crlr independently of VEGF signalling, and, conversely, via VEGF independently of Crlr, but that these signals converge again at the level of Notch (Fig. 7O).

Discussion

Hedgehog signalling plays a crucial role in inducing arterial fate in the zebrafish embryo. Elegant experiments by Lawson et al. (2002) revealed a hierarchy of signalling, initiated by Hh and leading, via the induction of VEGF, to activation of *hey2*/*gridlock* and Notch signalling to provide the final transcriptional output. More recently, an additional layer in this control has been suggested involving the Crlr receptor [19]. We have exploited the constitutive activation of the Hh pathway in double mutant *ptc1;ptc2* zebrafish embryos to explore further the relationships between Hh and VEGF in early vessel formation. In keeping with previous findings [17], we showed that activation of Hh leads to ectopic arterial gene expression, ultimately resulting in the absence of a functional circulatory loop. However, this endogenous hyper-activation of Hh signalling results in such strong repression of venous development that a correctly specified PCV fails to develop: rather, a second arterial vessel forms with an intact arterial marker signature, vessel sprouting and initiation of HSC gene expression.

An earlier role has been postulated for Hh signalling in guiding endothelial migration [11,26]. We have demonstrated that the levels of Hh signalling received by angioblasts are critical for their successful migration and that activation of the Hh pathway results in more severe defects in initial angioblast migration towards the midline than loss of Hh signalling. Previous studies have demonstrated that *smo* embryos exhibit a loss of arterial ECs and concomitant gain in venous ECs and it was proposed that Hh is required cell autonomously already within the PLM to regulate arterial-venous specificity [26]. Importantly, we find that in smo^{hi1640} mutants, the first wave of angioblast migration, which largely contributes to DA formation is not lost as has previously been reported [26]. The discrepancy between our findings and those of Williams et al., can most likely be explained by the higher resolution of the confocal imaging of angioblast migration used in our study. However, *smo* embryos lack arterial ECs, arguing that these two migratory waves are not differentially specified prior to migration. In line with this, the Hh receptors *ptc1* and *ptc2* are not expressed in the PLM [26,51] implying that cells of the PLM are unlikely to receive the Hh signal directly. From our high-resolution time-lapse movies, we suggest that Hh signalling is most important in the final stages of medial migration, since *smo*−/− angioblasts begin their

medial migration normally, yet fail to form a continuous endothelial cord as they reach the midline.

Interestingly, the arterial transformation of the ventral vessel leads to the generation of ISVs from this location, in addition to formation of atypical connections between the two axial vessels. Such connections have been observed in mutants with defects in arteriovenous specification and it is likely that separation of the two vessels requires them to have different molecular identities [14]. Considering the body of data implicating VEGF in arterial induction, we were initially surprised to find that mutation of *plcg1*, chemical ablation of VEGF signalling, or knockdown of the VEGF receptors failed to block normal and ectopic induction of arterial fates in double mutants. However, results from mice and also differences in phenotypic strength of VEGF and Hh pathway mutants [18,25], indicated that VEGF-independent functions of Hh signalling in these processes were likely. It is important to stress, however, that under normal circumstances VEGF is essential for arterial induction.

Although Nicoli and co-workers suggested that Crlr was induced by Hh in the somites and acted via VEGF, they could not exclude that direct effects of Crlr on ECs might occur. Indeed our experiments indicate that such direct effects are likely since downregulation of VEGF signalling is not sufficient to block arterial differentiation, arguing against a simple Hh-Crlr-VEGF pathway. If somitic VEGF was the sole effector acting on ECs to induce arterial fate, then inhibition of VEGF signalling in *ptc1;ptc2* mutants should have resulted in absence of arterial differentiation. Furthermore, it follows that *vegfa* overexpression would also be predicted to phenocopy the vascular defects of *ptc1;ptc2* mutants, a situation which did not occur (Fig. S6B and [17]).

The expression of *crlra* both in somites and ECs prompted us to analyse its potential role in bypassing a normal requirement for VEGF in double mutants. Indeed *crlra* expression was also induced in double mutants. Importantly, knock-down of *crlra* did not affect VEGF upregulation in the somites, thus it is likely that Crlr acts in the ECs in VEGF-inhibited double mutants. This finding raises several questions; most importantly how Crlr signalling is regulated. A recent report indicated that in certain cells CRLR might act to “transactivate” the VEGF receptor independently of the VEGF ligand [52]. However, these authors also show that the VEGF inhibitor we employed (SU5416) should block the action of both CRLR and VEGF receptor activation. Our data show that CRLR functions in the presence of SU5416, and thus this mechanism does not appear to be acting in zebrafish. A second simple assumption would be that signals via VEGF and Crlr could both independently induce arterial fate in ECs. This is not supported by experiments by us (Fig. S9) and others [19]. *crlr* overexpression is not sufficient to induce ectopic arterial fates in wild-types or rescue arterial fates in Hh signalling-deficient embryos. In contrast, VEGF has been shown to be an instructive factor with respect to arterial induction, and injection in wild-type or Hh signalling-deficient embryos can induce ectopic arteries (Fig. S6B and [17]). One interesting assumption concerning the role of Crlr may be that it acts to enhance or modify Hh signalling in ECs to induce arteries rather than act directly in the induction steps. We have looked at mRNA expression of the classical Hh target *ptc1* in *crlr* MO injected embryos but did not see changes (RNW, unpublished observations). Another possibility is that *crlr* overexpression by itself is not sufficient to increase signalling via this pathway and other crucial components of this pathway also need to be upregulated, such as RAMPs or Adrenomedullin ligands [53]. Then we have to assume that Hh activation in *ptc1;ptc2* mutants is not just upregulating *crlr* but also those other components required for its activation. We are currently evaluating this possibility.

The key outcome of Hh and VEGF signalling appears to be activation of Notch signalling. To further position the Crlr signalling pathway within this hierarchy we inhibited Notch

using a *Su(H)* morpholino capable of inhibiting the Notch pathway sufficiently to block artery formation [34]. We find that knock-down of *Su(H)* in *ptc1;ptc2* mutants can block artery formation, arguing that Crlr acts upstream of Notch. Thus, we suggest the model shown in Fig. 7O for the signalling hierarchies involved in artery formation. Our results show that while under normal circumstances VEGF is an essential signal for correct vessel patterning in the zebrafish embryo, in situations of elevated Hh signalling, Crlr can bypass this requirement. It may be interesting to evaluate whether similar mechanisms are at work in other settings, for example, in tumours where Hh signalling is activated. It has been reported that *crlr* downregulation inhibits tumour angiogenesis in a zebrafish xenograft model [19]. If this is a more widespread mechanism, inhibition of Crlr in addition to VEGF inhibition could be important to evaluate as a therapeutic strategy, not only for anti-cancer therapy, but also in the treatment of diseases such as diabetic retinopathy or macular degeneration. Furthermore, the remarkable conservation of the genetic hierarchies involved in arterial specification between zebrafish and mammals indicates that signalling via Crlr represents a strong candidate pathway for recently identified, but as yet uncharacterised, mechanisms of vessel patterning shown to be Hh-dependent and VEGF-independent [18].

Supplementary Material

Refer to Web version on PubMed Central for supplementary material.

Acknowledgments

We thank C. Pouget for reagents, assistance and critical reading of the manuscript, and W. Clements for sharing unpublished data. This work was supported by a Wellcome Trust Programme Grant 082962/Z/07/Z (PWI, FVE), the Medical Research Council (RP). The CDBG is supported by MRC Centre Grant G0700091 (PWI). The authors have declared that no conflict of interest exists.

References

1. Bertrand JY, Chi NC, Santoso B, Teng S, Stainier DY, Traver D. Haematopoietic stem cells derive directly from aortic endothelium during development. Nature. 2010; 464:108–111. [PubMed: 20154733]
2. Kissa K, Herbomel P. Blood stem cells emerge from aortic endothelium by a novel type of cell transition. Nature. 2010; 464:112–115. [PubMed: 20154732]
3. Boisset JC, van Cappellen W, Andrieu-Soler C, Galjart N, Dzierzak E, Robin C. In vivo imaging of haematopoietic cells emerging from the mouse aortic endothelium. Nature. 2010; 464:116–120. [PubMed: 20154729]
4. Vogeli KM, Jin SW, Martin GR, Stainier DY. A common progenitor for haematopoietic and endothelial lineages in the zebrafish gastrula. Nature. 2006; 443:337–339. [PubMed: 16988712]
5. Fouquet B, Weinstein BM, Serluca FC, Fishman MC. Vessel patterning in the embryo of the zebrafish: guidance by notochord. Dev Biol. 1997; 183:37–48. [PubMed: 9119113]
6. Wang HU, Chen ZF, Anderson DJ. Molecular distinction and angiogenic interaction between embryonic arteries and veins revealed by ephrin-B2 and its receptor Eph-B4. Cell. 1998; 93:741–753. [PubMed: 9630219]
7. Lawson ND, Weinstein BM. Arteries and veins: making a difference with zebrafish. Nat Rev Genet. 2002; 3:674–682. [PubMed: 12209142]
8. Zhong TP, Childs S, Leu JP, Fishman MC. Gridlock signalling pathway fashions the first embryonic artery. Nature. 2001; 414:216–220. [PubMed: 11700560]
9. Lawson ND, Scheer N, Pham VN, et al. Notch signaling is required for arterial-venous differentiation during embryonic vascular development. Development. 2001; 128:3675–3683. [PubMed: 11585794]
10. Jin SW, Beis D, Mitchell T, Chen JN, Stainier DY. Cellular and molecular analyses of vascular tube and lumen formation in zebrafish. Development. 2005; 132:5199–5209. [PubMed: 16251212]

11. Gering M, Patient R. Hedgehog signaling is required for adult blood stem cell formation in zebrafish embryos. Dev Cell. 2005; 8:389–400. [PubMed: 15737934]
12. Hong CC, Peterson QP, Hong JY, Peterson RT. Artery/vein specification is governed by opposing phosphatidylinositol-3 kinase and MAP kinase/ERK signaling. Curr Biol. 2006; 16:1366–1372. [PubMed: 16824925]
13. Herbert SP, Huisken J, Kim TN, et al. Arterial-venous segregation by selective cell sprouting: an alternative mode of blood vessel formation. Science. 2009; 326:294–298. [PubMed: 19815777]
14. Lin FJ, Tsai MJ, Tsai SY. Artery and vein formation: a tug of war between different forces. EMBO Rep. 2007; 8:920–924. [PubMed: 17906673]
15. Zhong TP, Rosenberg M, Mohideen MA, Weinstein B, Fishman MC. gridlock, an HLH gene required for assembly of the aorta in zebrafish. Science. 2000; 287:1820–1824. [PubMed: 10710309]
16. Rowlinson JM, Gering M. Hey2 acts upstream of Notch in hematopoietic stem cell specification in zebrafish embryos. Blood. 116:2046–2056. [PubMed: 20511544]
17. Lawson ND, Vogel AM, Weinstein BM. sonic hedgehog and vascular endothelial growth factor act upstream of the Notch pathway during arterial endothelial differentiation. Dev Cell. 2002; 3:127–136. [PubMed: 12110173]
18. Coultas L, Nieuwenhuis E, Anderson GA, et al. Hedgehog regulates distinct vascular patterning events through VEGF-dependent and -independent mechanisms. Blood. 2010; 116:653–660. [PubMed: 20339091]
19. Nicoli S, Tobia C, Gualandi L, De Sena G, Presta M. Calcitonin receptor-like receptor guides arterial differentiation in zebrafish. Blood. 2008; 111:4965–4972. [PubMed: 18326814]
20. Lawson ND, Mugford JW, Diamond BA, Weinstein BM. phospholipase C gamma-1 is required downstream of vascular endothelial growth factor during arterial development. Genes Dev. 2003; 17:1346–1351. [PubMed: 12782653]
21. Habeck H, Odenthal J, Walderich B, Maischein H, Schulte-Merker S. Analysis of a zebrafish VEGF receptor mutant reveals specific disruption of angiogenesis. Curr Biol. 2002; 12:1405–1412. [PubMed: 12194822]
22. Covassin LD, Villefranc JA, Kacergis MC, Weinstein BM, Lawson ND. Distinct genetic interactions between multiple Vegf receptors are required for development of different blood vessel types in zebrafish. Proc Natl Acad Sci U S A. 2006; 103:6554–6559. [PubMed: 16617120]
23. You LR, Lin FJ, Lee CT, DeMayo FJ, Tsai MJ, Tsai SY. Suppression of Notch signalling by the COUP-TFII transcription factor regulates vein identity. Nature. 2005; 435:98–104. [PubMed: 15875024]
24. Vokes SA, Yatskievych TA, Heimark RL, et al. Hedgehog signaling is essential for endothelial tube formation during vasculogenesis. Development. 2004; 131:4371–4380. [PubMed: 15294868]
25. Pola R, Ling LE, Silver M, et al. The morphogen Sonic hedgehog is an indirect angiogenic agent upregulating two families of angiogenic growth factors. Nat Med. 2001; 7:706–711. [PubMed: 11385508]
26. Williams C, Kim SH, Ni TT, et al. Hedgehog signaling induces arterial endothelial cell formation by repressing venous cell fate. Dev Biol. 2010; 341:196–204. [PubMed: 20193674]
27. Koudijs MJ, den Broeder MJ, Groot E, van Eeden FJ. Genetic analysis of the two zebrafish patched homologues identifies novel roles for the hedgehog signaling pathway. BMC Dev Biol. 2008; 8:15. [PubMed: 18284698]
28. Koudijs MJ, den Broeder MJ, Keijser A, et al. The zebrafish mutants dre, uki, and lep encode negative regulators of the hedgehog signaling pathway. PLoS Genet. 2005; 1:e19. [PubMed: 16121254]
29. Westerfield, M. The zebrafish book. A guide for the laboratory use of zebrafish (Danio rerio). Univ. of Oregon Press; Eugene: 1993.
30. Wilkinson RN, Pouget C, Gering M, et al. Hedgehog and Bmp polarize hematopoietic stem cell emergence in the zebrafish dorsal aorta. Dev Cell. 2009; 16:909–916. [PubMed: 19531361]
31. Kwan KM, Fujimoto E, Grabher C, et al. The Tol2kit: a multisite gateway-based construction kit for Tol2 transposon transgenesis constructs. Dev Dyn. 2007; 236:3088–3099. [PubMed: 17937395]

32. Villefranc JA, Amigo J, Lawson ND. Gateway compatible vectors for analysis of gene function in the zebrafish. Dev Dyn. 2007; 236:3077–3087. [PubMed: 17948311]
33. Hammerschmidt M, Bitgood MJ, McMahon AP. Protein kinase A is a common negative regulator of Hedgehog signaling in the vertebrate embryo. Genes Dev. 1996; 10:647–658. [PubMed: 8598293]
34. Echeverri K, Oates AC. Coordination of symmetric cyclic gene expression during somitogenesis by Suppressor of Hairless involves regulation of retinoic acid catabolism. Dev Biol. 2007; 301:388–403. [PubMed: 17098223]
35. Bahary N, Goishi K, Stuckenholz C, et al. Duplicate VegfA genes and orthologues of the KDR receptor tyrosine kinase family mediate vascular development in the zebrafish. Blood. 2007; 110:3627–3636. [PubMed: 17698971]
36. Lawson ND, Weinstein BM. In vivo imaging of embryonic vascular development using transgenic zebrafish. Dev Biol. 2002; 248:307–318. [PubMed: 12167406]
37. Traver D, Paw BH, Poss KD, Penberthy WT, Lin S, Zon LI. Transplantation and in vivo imaging of multilineage engraftment in zebrafish bloodless mutants. Nat Immunol. 2003; 4:1238–1246. [PubMed: 14608381]
38. Chen W, Burgess S, Hopkins N. Analysis of the zebrafish smoothened mutant reveals conserved and divergent functions of hedgehog activity. Development. 2001; 128:2385–2396. [PubMed: 11493557]
39. Isogai S, Horiguchi M, Weinstein BM. The vascular anatomy of the developing zebrafish: an atlas of embryonic and early larval development. Dev Biol. 2001; 230:278–301. [PubMed: 11161578]
40. Bussmann J, Bos FL, Urasaki A, Kawakami K, Duckers HJ, Schulte-Merker S. Arteries provide essential guidance cues for lymphatic endothelial cells in the zebrafish trunk. Development. 2010; 137:2653–2657. [PubMed: 20610484]
41. Tucker B, Hepperle C, Kortschak D, et al. Zebrafish Angiotensin II Receptor-like 1a (agtrl1a) is expressed in migrating hypoblast, vasculature, and in multiple embryonic epithelia. Gene Expr Patterns. 2007; 7:258–265. [PubMed: 17085078]
42. Burns CE, Traver D, Mayhall E, Shepard JL, Zon LI. Hematopoietic stem cell fate is established by the Notch-Runx pathway. Genes Dev. 2005; 19:2331–2342. [PubMed: 16166372]
43. Kalev-Zylinska ML, Horsfield JA, Flores MV, et al. Runx1 is required for zebrafish blood and vessel development and expression of a human RUNX1-CBF2T1 transgene advances a model for studies of leukemogenesis. Development. 2002; 129:2015–2030. [PubMed: 11934867]
44. Clements WK, Kim AD, Ong KG, Moore JC, Lawson ND, Traver D. A somitic Wnt16/Notch pathway specifies haematopoietic stem cells. Nature. 2011; 474:220–224. [PubMed: 21654806]
45. Sinha S, Chen JK. Purmorphamine activates the Hedgehog pathway by targeting Smoothened. Nat Chem Biol. 2006; 2:29–30. [PubMed: 16408088]
46. Covassin LD, Siekmann AF, Kacergis MC, et al. A genetic screen for vascular mutants in zebrafish reveals dynamic roles for Vegf/Plcg1 signaling during artery development. Dev Biol. 2009; 329:212–226. [PubMed: 19269286]
47. Nasevicius A, Larson J, Ekker SC. Distinct requirements for zebrafish angiogenesis revealed by a VEGF-A morphant. Yeast. 2000; 17:294–301. [PubMed: 11119306]
48. Vajkoczy P, Menger MD, Vollmar B, et al. Inhibition of tumor growth, angiogenesis, and microcirculation by the novel Flk-1 inhibitor SU5416 as assessed by intravital multi-fluorescence videomicroscopy. Neoplasia. 1999; 1:31–41. [PubMed: 10935468]
49. Serbedzija GN, Flynn E, Willett CE. Zebrafish angiogenesis: a new model for drug screening. Angiogenesis. 1999; 3:353–359. [PubMed: 14517415]
50. Fortini ME, Artavanis-Tsakonas S. The suppressor of hairless protein participates in notch receptor signaling. Cell. 1994; 79:273–282. [PubMed: 7954795]
51. Lewis KE, Concordet JP, Ingham PW. Characterisation of a second patched gene in the zebrafish Danio rerio and the differential response of patched genes to Hedgehog signalling. Dev Biol. 1999; 208:14–29. [PubMed: 10075838]
52. Guidolin D, Albertin G, Spinazzi R, et al. Adrenomedullin stimulates angiogenic response in cultured human vascular endothelial cells: involvement of the vascular endothelial growth factor receptor 2. Peptides. 2008; 29:2013–2023. [PubMed: 18692535]

53. Gibbons C, Dackor R, Dunworth W, Fritz-Six K, Caron KM. Receptor activity-modifying proteins: RAMPing up adrenomedullin signaling. Mol Endocrinol. 2007; 21:783–796. [PubMed: 17053041]

Europe PMC Funders Author Manuscripts

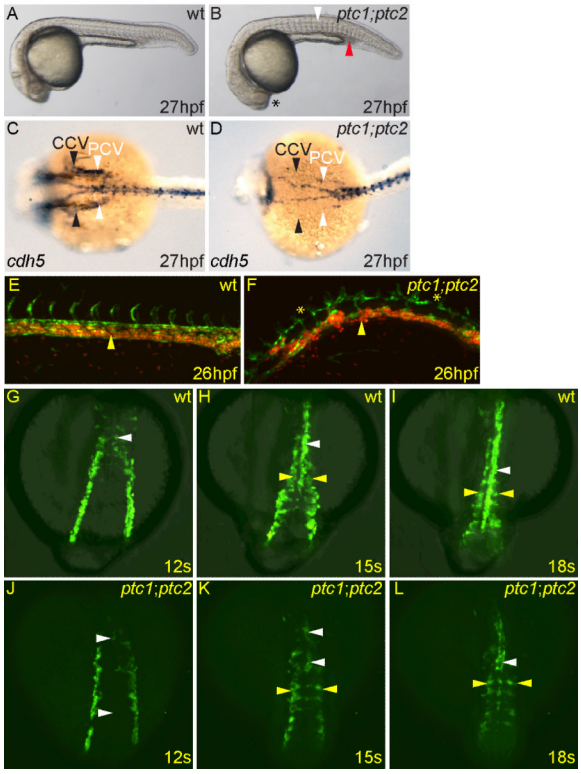

Figure 1. Zebrafish *ptc1;ptc2* double mutants fail to establish circulation and exhibit multiple endothelial defects and defective angioblast migration

A, **B**) *ptc1*;*ptc2* mutant (**B**) embryos at 27hpf showed somitic flattening (white arrowhead) and loss of lens (asterisk). *ptc1*;*ptc2* embryos showed non-circulating primitive erythrocytes in the posterior ICM (red arrowhead). **C, D)** *cdh5* expression in *ptc1*;*ptc2* mutants (**D**) revealed defective formation of the CCV/DC (black arrowheads) and PCV (white arrowheads) compared to *wild-type* (**C**). **E, F**) Confocal image of trunk vasculature in Tg(*fli1a:EGFP*)*y1*;Tg(*gata1:dsred*)*sd2*/+ (**E**) and Tg(*gata1:dsred*)*sd2*/+;*ptc1;ptc2* (**F**) embryos, anterior to the left, posterior right. The primary vasculature formed normally in Tg(*fli1a:EGFP*)*y1*;Tg(*gata1:dsred*)*sd2*/+ embryos, and circulation commenced normally (yellow arrowhead and Movie S1), whilst Tg(*fli1a:EGFP*)*y1*;Tg(*gata1:dsred*)*sd2*/+;*ptc1;ptc2* embryos had disorganised vasculature, axial vessels were non-continuous along their A-P axis (asterisks) and embryos lacked circulation (yellow arrowhead and Movie S2). **G-L**) Confocal images using a Tg(*fli1a:EGFP*)*y1*/+ background to visualise migrating angioblasts in indicated genetic backgrounds. Dorsal views are shown. **G-I**) Normal angioblast migration in Tg(*fli1a:EGFP*)*y1*/+ embryos. (**J-L**) Fewer angioblasts migrated to the midline in Tg(*fli1a:EGFP*)*y1*/+;*ptc1;ptc2* embryos and formed a discontinuous endothelial cord by 18s (Movie S3 and white arrowheads). Angioblasts were present in more lateral positions (Movie S4 and L, yellow arrowheads) than in controls at the corresponding stage (**I**, yellow arrrowheads). **CCV** common cardinal vein, **PLM** posterior lateral mesoderm, **ICM** intermediate cell mass.

Europe PMC Funders Author Manuscripts

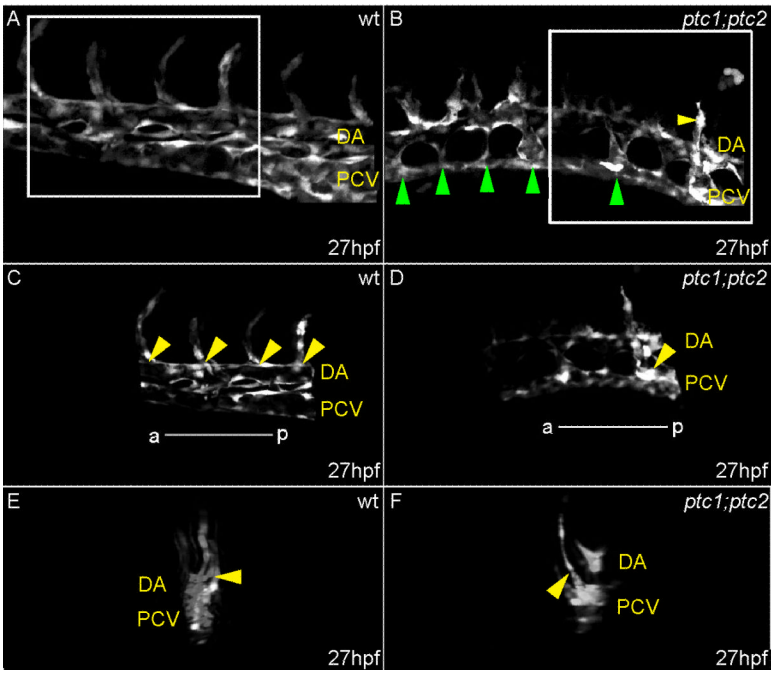

Figure 2. *ptc1;ptc2* mutants exhibit precocious vessel sprouting from the posterior cardinal vein

Confocal images of developing trunk vasculature in Tg(*fli1a:EGFP*)*y1*/+ (**A, C, E**) and Tg(*fli1a:EGFP*)*y1*/+;*ptc1*;*ptc2* embryos at 27hpf (**B, D, F**), anterior is left, posterior right. **A**) Normal trunk vasculature. Highlighted area is shown in panel C. **B**) Endothelial connections between the DA and PCV were present in Tg(*fli1a:EGFP*)*y1*/+;*ptc1*;*ptc2* embryos (grey arrowheads) and ectopic vessel sprouts arising from PCV were present (**B**, **D white arrowheads)**. Highlighted area is shown in panel d. 3D reconstruction showing transverse plane of embryo shown in panels A, C (**E**) and embryo shown in panels B**, D** (**F**) shows the sprouting capacity of ECs in the PCV region in *ptc1*;*ptc2* mutants (white arrowhead).

Europe PMC Funders Author Manuscripts

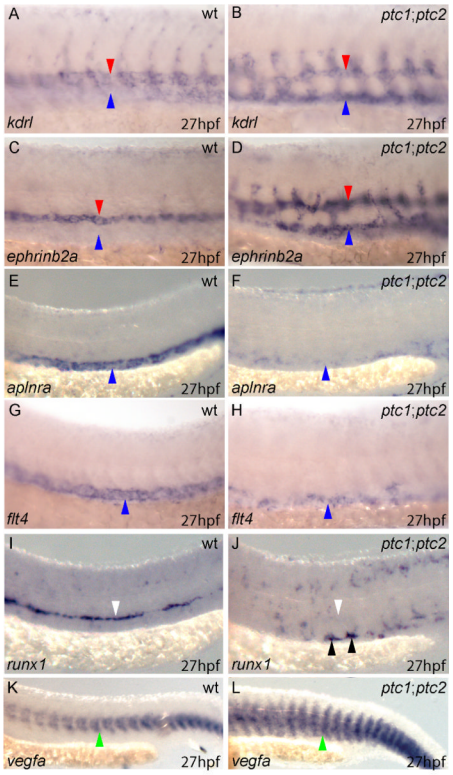

Figure 3. *ptc1*; *ptc2* mutants exhibit ectopic arterial differentiation at the expense of venous differentiation, resulting in conversion of the PCV into a second artery

Lateral views of trunk region are shown, oriented anterior to left, posterior right. **A**) *kdrl* exhibited arterial preference in wild-type embryos (red arrowheads), but was present ectopically in the PCV in *ptc1;ptc2* embryos (**B,** blue arrowheads). **C**) *ephrinb2a* was restricted to the DA in wild-type embryos (red arrowhead) but present ectopically in the PCV in *ptc1;ptc2* embryos (blue arrowheads). **E**) *aplnra* and *flt4* (**G**) expression was restricted to the PCV in wild-type embryos (blue arrowheads) and downregulated in *ptc1;ptc2* embryos (**F**, **H**, blue arrowheads). **I**) *runx1* was restricted to the DA in wild-type embryos (white arrowhead), downregulated in the DA of *ptc1;ptc2* embryos (**J,** white arrowhead) and ectopically expressed in the PCV of *ptc1;ptc2* embryos (**J**, black arrowheads). **K**) Increased trunk *vegfa* expression was present in *ptc1;ptc2* embryos (**L**, green arrowhead) in comparison to wild-type (**K**, green arrowhead).

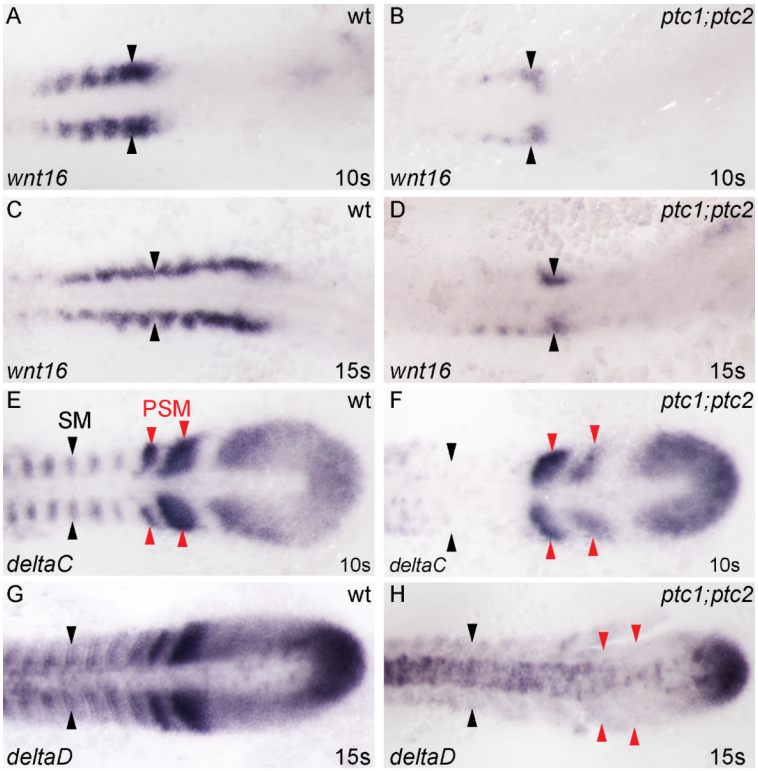

Figure 4. Somitic *wnt16-deltaC/deltaD* signalling required for HSC specification is abrogated in *ptc1;ptc2* mutants

Zebrafish flat mounts are shown with anterior to the left and posterior to the right. **A, B**) somitic *wnt16* expression is strongly downregulated in *ptc1;ptc2* embryos at 10s (**B**, black arrowheads) and this downregulation persisted at 15s stage (**C**, **D** black arrowheads). **E**, **F**) Expression of *deltaC* was absent from the somitic mesoderm (SM) of *ptc1;ptc2* embryos (**F**, black arrowheads), but was present within the pre-somitic mesoderm (PSM) (**F**, grey arrowheads). **G**, **H**) *deltaD* expression was strongly downregulated within the SM (**H**, black arrowheads) and PSM (**H**, grey arrowheads) of *ptc1;ptc2* embryos.

Europe PMC Funders Author Manuscripts

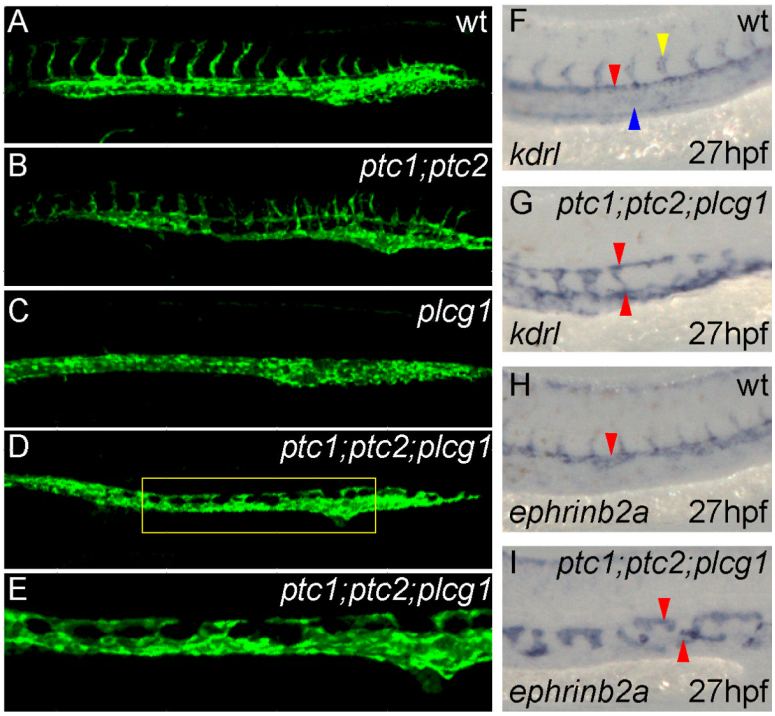

Figure 5. Arterial specification occurs independently of VEGF signalling in *ptc1;ptc2;plcg1* triple mutants

(**A-E**) Tg(*fli1a:EGFP)y1*/+;*ptc1;ptc2* embryos formed two separate vessels, both with sprouting capacity (**B**), whilst Tg(*fli1a:EGFP)y1*/+;*plcg1*^{t26480} embryos formed a single vessel without ISV sprouts lacking arterial gene expression (data not shown)(**C**). Two separate vessels were present in triple mutant embryos (**D**, zoomed view in **E**), but no ISVs formed. *kdrl* (**F**, **G**) and *ephrinb2a* (**H**, **I**) expression indicated that the DA remained duplicated in the triple mutants, albeit with fewer cells.

Europe PMC Funders Author Manuscripts

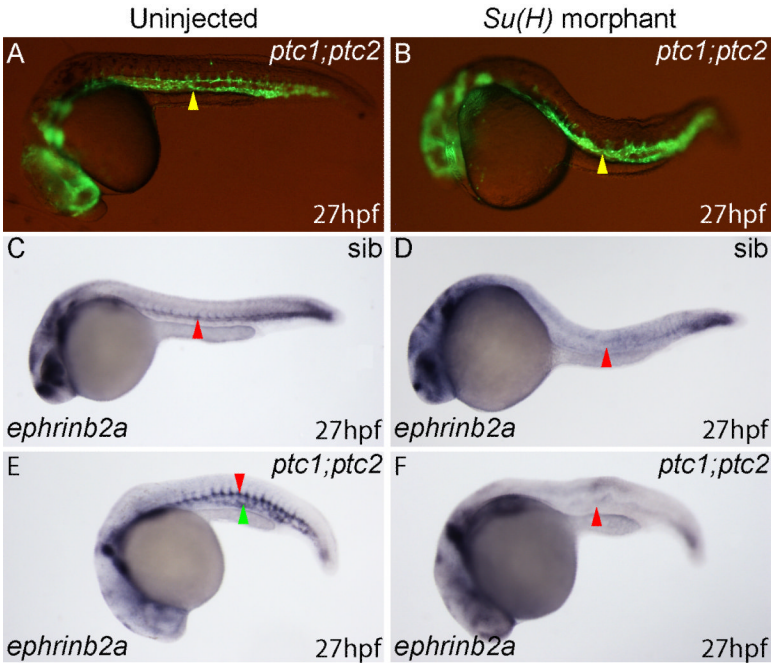

Figure 6. Arterial specification in *ptc1;ptc2* mutants is dependent upon Notch signalling

A) Tg(*fli1a:EGFP*)*y1*/+;*ptc1;ptc2* embryos exhibit blood vessel formation (**B**, yellow arrowhead) (n= 15/230) even following Su(H) morpholino injection (**B**, yellow arrowhead) (n= 5/95) **C)** Normal DA *ephrinb2a* expression in uninjected non-double mutant embryos (**C**, red arrowhead) (n=157/167) **D**) Loss of *ephrinb2a* in DA of non-double mutant *Su(H)* morphants (red arrowhead) (n=159/180) **E**) Increased (red arrowhead), ectopic (green arrowhead) *ephrinb2a* expression in uninjected *ptc1;ptc2* embryos (n=10/167) **F**) Loss of *ephrinb2a* in DA of *ptc1;ptc2 Su(H)* morphants (n=16/180)

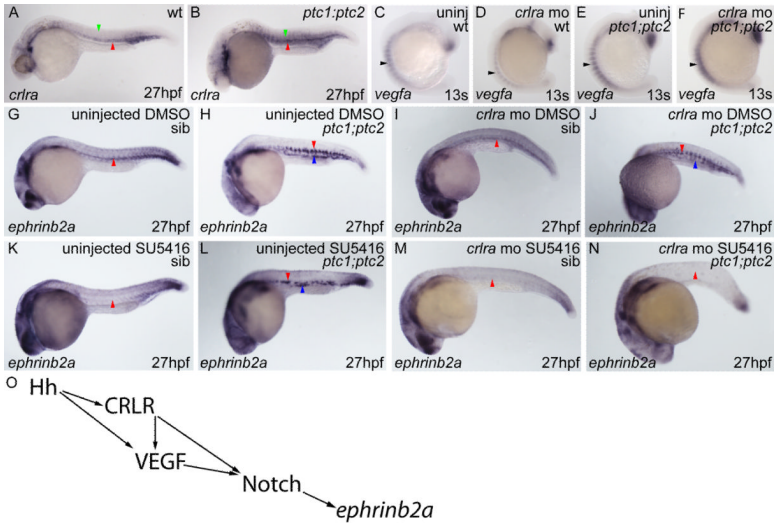

Figure 7. Knockdown of *crlrla* in combination with VEGF inhibition prevents arterial differentiation in *ptc1;ptc2* mutants

A) Wild-type somitic (green arrowhead) and DA *crlra* expression (red arrowhead) **B**) Increased somitic (green arrowhead) and DA (red arrowhead) *crlra* expression in *ptc1;ptc2* embryos. **C**) normal somitic *crlra* expression in uninjected wild type non-double mutant embryos (arrowhead) (n=58/66) **D**) Decreased somitic *crlra* expression in non-double mutant *crlra* morphants (n=58/71). **E, F**) No difference in *crlra* expression (arrowheads) was detected between uninjected (n=5/66) and *crlra* morphant (n=4/71) *ptc1;ptc2* embryos. Uninjected wild-type sibs treated with SU5416 from tailbud until collection exhibited total absence of vascular *ephrinb2a* expression (**K**, red arrowhead) (n=40/50) compared to controls (**G**, red arrowhead) (n=46/49). SU5416 treated *ptc1;ptc2* mutants showed increased *ephrinb2a* (L, red arrowhead) and ectopic expression in PCV region (**L**, blue arrowhead) (n=4/50), as did uninjected *ptc1;ptc2* mutants (**H**, red and blue arrowheads) (n=3/49). Uninjected SU5416 treated *ptc1;ptc2* embryos exhibited no vessel sprouting in comparison to DMSO treated *ptc1;ptc2* embryos. *ephrinb2a* expression was downregulated in the DA of non-double mutant *crlra* morphants treated with DMSO (**I**, red arrowhead) (n=78/96), whilst non-double mutant *crlra* morphants treated with SU5416 exhibited a loss of vascular *ephrinb2a* expression (**M**, red arrowhead) (n=165/183). *ptc1;ptc2 crlra* morphants treated with DMSO showed strong *ephrinb2a* expression (**J**, red arrowhead), which was present ectopically in the region of the PCV (**J**, blue arrowhead) (n=8/96), whilst vascular *ephrinb2a* was absent in *ptc1;ptc2 crlra* morphants treated with SU5416 (**N,** red arrowhead) (n=10/186). **O**) Proposed model for arterial differentiation.

Europe PMC Funders Author Manuscripts